Research Article

Influence of spinal cord injury on core regions of motor function

https://doi.org/10.4103/1673-5374.293158

Received: February 14, 2020

Peer review started: February 25, 2020

Accepted: April 7, 2020

Published online: September 22, 2020

Xiao-Yan Shen[1, 2, *], Chun-Ling Tao[1], Lei Ma[1], Jia-Huan Shen[1], Zhi-Ling Li[1], Zhi-Gong Wang[2, 3], Xiao-Ying Lü[4]

Graphical Abstract *Spinal cord injury causes the migration of motor function regions*

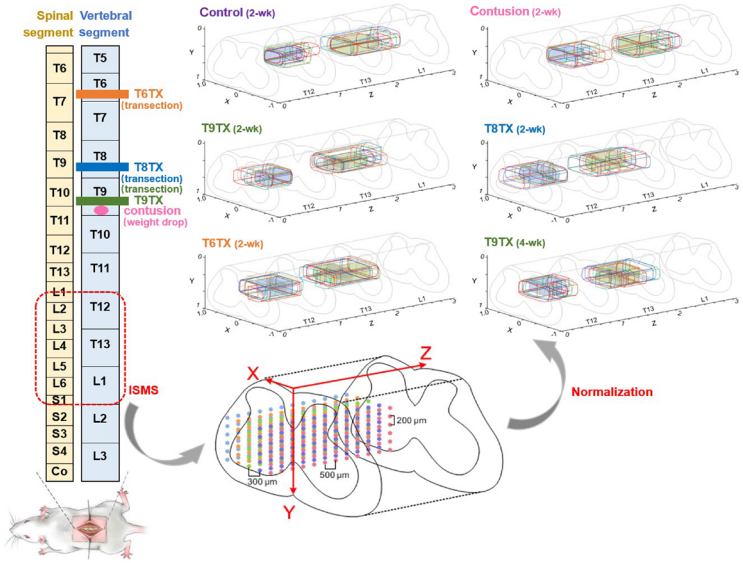

Abstract

Functional electrical stimulation is an effective way to rebuild hindlimb motor function after spinal cord injury. However, no site map exists to serve as a reference for implanting stimulator electrodes. In this study, rat models of thoracic spinal nerve 9 contusion were established by a heavy-impact method and rat models of T6/8/9 spinal cord injury were established by a transection method. Intraspinal microstimulation was performed to record motion types, site coordinates, and threshold currents induced by stimulation. After transection (complete injury), the core region of hip flexion migrated from the T13 to T12 vertebral segment, and the core region of hip extension migrated from the L1 to T13 vertebral segment. Migration was affected by post-transection time, but not transection segment. Moreover, the longer the post-transection time, the longer the distance of migration. This study provides a reference for spinal electrode implantation after spinal cord injury. This study was approved by the Institutional Animal Care and Use Committee of Nantong University, China (approval No. 20190225-008) on February 26, 2019.

Key Words: model; motor; neurological function; rat; recovery; repair; spinal cord injury

Chinese Library Classification No. R454; R741; R312

Introduction

Spinal cord injury (SCI) refers to structural or functional injury of the spinal cord resulting in movement, sensation, and autonomic dysfunction below the level of injury (Nakae et al., 2011). Whether the cause is trauma or disease, SCI has a high disability rate. The number of people suffering from SCI in China has exceeded one million and is surging at a rate of 140,000 annually (Zhou, 2013). In 2016, there were about 282,000 people suffering from SCI in the United States (Borrell et al., 2017), while the total number of people with SCI has exceeded 3 million worldwide (Nakae et al., 2011). Because it is difficult to recover injured neurons and restore conduction function of axons, treatment of SCI has become a worldwide problem (Borton et al., 2014).

[1]School of Information Science and Technology, Nantong University, Nantong, Jiangsu Province, China; [2]Co-innovation Center of Neuroregeneration, Nantong University, Nantong, Jiangsu Province, China; [3]Institute of RF and OE-ICs, Southeast University, Nanjing, Jiangsu Province, China; [4]State Key Laboratory of Bioelectronics, Southeast University, Nanjing, Jiangsu Province, China

*Correspondence to: Xiao-Yan Shen, PhD, xiaoyansho@ntu.edu.cn.

https://orcid.org/0000-0003-4551-186X (Xiao-Yan Shen)

Funding: *This work was supported by the National Natural Science Foundation of China, No. 61534003 (to ZGW), 81371663 (to XYS); Opening Project of State Key Laboratory of Bioelectronics in Southeast University (to XYS); the "226 Engineering" Research Project of Nantong Government (to XYS); "Six Talent Peaks" Project, No. SWYY-116 (to XYS) and Postgraduate Research & Practice Innovation Program of Jiangsu Province, No. KYCX18_2424 (to CLT).*

How to cite this article: *Shen XY, Tao CL, Ma L, Shen JH, Li ZL, Wang ZG, Lü XY (2021) Influence of spinal cord injury on core regions of motor function. Neural Regen Res 16(3):567-572.*

Intraspinal microstimulation, a new form of functional electrical stimulation, exhibits potential to restore spinal motor function (Saigal et al., 2004). Studies of intraspinal microstimulation on the spinal cords of cats demonstrated that stimulating different lumbosacral regions can produce single muscle activity and selectively induce the required motion (Bamford et al., 2011; Holinski et al., 2011). Jackson and Zimmermann (2012) observed that if the spinal motor neuron network below the injury plane remains intact, it can activate its motor function during electrical stimulation. In addition, researchers have successfully rebuilt nerve function remotely in toads with microelectronic neural bridge technology (Wang et al., 2005; Shen et al., 2010).

Based on these findings, we developed a microelectronic neural bridge to repair spinal cord function (Shen et al., 2012). The main idea was to implant a microelectronic chip in the injured point, collect the motion control signal from the cerebral cortex, and then process and output this signal to the descending pathway to realize restoration of the body function (Huang et al., 2016). However, to successfully implement this new strategy for restoration of motor function in SCI, it is crucial to determine the electrode implantation region in the spinal cord and accurately stimulate the distal spinal nerve bundle. Currently, there is no reference map of motor stimulation sites for animal experiments; instead, most studies use multiple stimulations to identify desired sites, causing secondary damage to the spinal cord (Bamford et al., 2017). Furthermore, whether SCI changes the spinal function region controlling hindlimb motion and whether different conditions of SCI elicit different results are worth examining. Therefore, the present study evaluated the influence of SCI on spinal motor function regions in rats from different SCI models, transection segments, and post-transection times.

Materials and Methods

Animals

All protocols involving the use of animals in this study were approved by the Institutional Animal Care and Use Committee of Nantong University, China (Approval No. 20190225-008) on February 26, 2019. A total of 36 Sprague-Dawley rats (both sexes, weighing ~250 g) were purchased from the Experimental Animal Center of Nantong University (License No. SYXK (Su) 2017-0046). All rats were randomly divided into control, contusion, and transection groups. In the control group (n = 6), rats were fed normally for 2 weeks. In the contusion group (n = 6), the thoracic spinal nerve 9 (T9) segment of rats was injured with a weight drop, followed by 2 weeks of normal feeding. Rats in transection groups underwent T6/T8/T9 transection, and were randomly divided into four subgroups (n = 6): T9TX2, T9TX4, T8TX, and T6TX. The transection site of rats in T9TX2 and T9TX4 subgroups was at T9, followed by 2 and 4 weeks of normal feeding. Transection sites in T8TX and T6TX subgroups were at T8 and T6, respectively, followed by 2 weeks of normal feeding. An experimental flow chart is shown in **Figure 1**.

Preparation of SCI model

Rats were anesthetized by intraperitoneal injection of compound anesthetic (0.2 mL/100 g) containing 4.25 g chloral hydrate, 2.12 g magnesium sulfate, 0.88 g sodium pentobarbital, 14.25 mL anhydrous alcohol, 33.80 mL 1,2-propanediol, and 51.95 mL double distilled water. Vertebral segments that needed to be opened were determined, and about 5 mm of the spinal cord was exposed by cutting off the laminae.

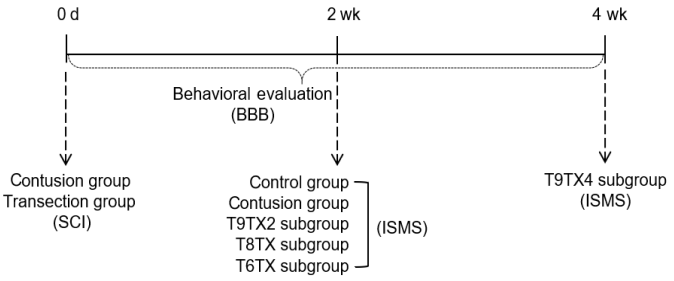

Figure 1 | **Flow chart of the study.**
Control group: Rats were fed normally for 2 weeks; Contusion group: T9 segment was injured with weight drop, followed by 2 weeks of normal feeding; T9TX2, T8TX, T6TX, and T9TX4 groups: T6/T8/T9 transection, followed by 2 or 4 weeks of normal feeding. BBB: Basso-Beattie-Bresnahan locomotor rating scale; ISMS: intraspinal microstimulation; SCI: spinal cord injury.

Contusion group

To imitate incomplete spinal cord injury, the exposed spinal cord was struck at the middle by a MASCIS Impactor Model-III (Rutgers, New Brunswick, NJ, USA) (Basso et al., 1996). The diameter of the impact head was 2.5 mm, its weight was 10 g, and the impact height was 6.25 mm.

Transection group

To imitate complete injury, about 2 mm of the spinal cord was removed with a blade from the middle of the exposed spinal cord (the blade should touch the anterior and lateral bone surface of the vertebra). Compression hemostasis was adopted during surgery, and a hemostatic sponge was used to fill the lesion. Finally, the muscles and skin were sutured and thoroughly washed with saline (Song et al., 2015).

After the operation, rats were individually raised with free access to food. The temperature was controlled at 28°C, and litters were cleaned daily. The bladder of each rat was massage to facilitate urination 2–3 times a day until the urinary reflex function was basically restored. Rats were intraperitoneally injected with 1×10^5 units of gentamicin sulfate (Justwore Pharmaceutical Co., Yantai, Shandong Province, China) for anti-infection for 3 days after surgery.

Behavioral evaluation

The motor function of rat hindlimbs in each group was scored at the open site before and 0, 1, 3, 7, 10, and 14 days after surgery. The Basso-Beattie-Bresnahan (BBB) locomotor rating scale was used to independently assess animals by a double-blind method (Basso et al., 1996; Song et al., 2015). Scores ranging from 0–21 represent no hindlimb movement to normal gait movement. Rats were preoperatively trained to locomote in an open field, which was a rectangular platform with a smooth, nonslip floor (2-m^2 area). Once a rat walked continuously in the open field, two examiners conducted a 4-minute evaluation and recorded their scores. The average score of the two examiners was treated as the evaluation result.

Determination of core regions of motor function

Stimulating electrode and parameters

The stimulating electrode was a tungsten single electrode (WE30030.5A3; MicroProbes, Gaithersburg, MD, USA), with a 1-μm diameter and 1.5-MΩ impedance. Recording and reference electrodes were self-made acupuncture needle electrodes with 0.16-mm diameters.

The biphasic stimulation pulse sequence [can balance positive and negative charges during stimulation and reduce electrochemical damage (Griffin et al., 2009; Musienko et al., 2009)] was generated by a Master-9 pulse stimulator (AMPI, Wollongong, Australia). The negative pulse width was 0.2 ms, the positive pulse width was 2 ms, and the pulse interval was 27.8 ms. The frequency was 40 Hz, with a stimulation duration of 1.2 seconds and stimulation interval of 2.8 seconds. The electromyogram (EMG) signal was acquired by PowerLab (ML870; ADI, Norwood, MA, USA) with a sampling rate of 2 kHz, differential amplification, and bandpass filtering of 20–1000 Hz.

Surgical procedure

Rats were anesthetized by intraperitoneal injection of compound anesthetic (0.2 mL/100 g), as described above. The T12–L2 vertebral segments were identified and exposed. The length of each vertebral segment was measured for normalization and marked on the muscles. The laminae were removed to expose the corresponding spinal cord, meanwhile ensuring that the endorachis was intact. The widest position of the intumescentia lumbalis (D) was measured for normalization. The spinal cord was covered with saline gauze to maintain activity. Bipolar electrodes were implanted in the hindlimb muscles (biceps femoris and rectus femoris) of the rat. The reference electrode was implanted adjacent to the paraspinal muscle.

Each rat was fixed on the fully automatic brain stereotaxic instrument (51700; Stoelting, Wood Dale, IL, USA) and fixed with a spinal adapter. As shown in **Figure 2**, the stimulus waveform was generated by the signal generator (Master-9) and output to the tungsten wire electrode, which was fixed on the stereotaxic instrument through the stimulus isolator (ISO-Flex, AMPI). Simultaneously, the EMG signal was recorded by PowerLab to confirm whether the con-traction of relevant muscles was induced. **Figure 3** shows recorded EMG signals. Taking the posterior median sulcus of the spinal cord as the coordinate origin, the electrode was moved at a 300-μm interval along the *X*-axis in the medi-olateral direction, a 200-μm interval along the *Y*-axis in the dorsoventral direction, and a 500-μm interval along the *Z*-axis in the rostrocaudal direction (the stimulation range was the gray matter of spinal cord and its adjacent location) (**Figure 4**). The stimulation current was adjusted by the stimulation isolator to determine the threshold current capable of inducing the motion (Chen et al., 2017). Simultaneously, site coordinates capable of inducing hip flexion and hip extension were recorded.

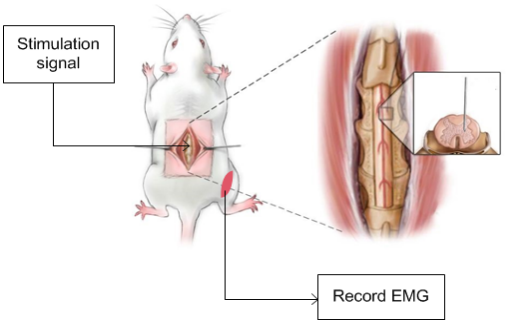

Figure 2 | **Determination of core motor function regions.**
The stimulus waveform was generated by the signal generator (Master-9) and output to the spinal cord. Simultaneously, the electromyogram (EMG) signal was recorded by PowerLab to confirm whether the contraction of relevant muscles was induced.

Site coordinate normalization

The geometric parameters of spinal cord stimulation sites must be normalized to reduce variances in the length and transverse diameter of spinal cords between individuals. The normalization method was as follows: the mediolateral direction *X* was normalized by D/2, the dorsoventral direction *Y* was normalized by D (to avoid measuring of the dorsoventral diameter *in vivo*, which causes greater damage) (Capogrosso et al., 2016), and the rostrocaudal direction *Z* was normalized by the length of spine segments. After normalization, the distribution maps of spinal motor function in each rat were drawn in the same coordinate system.

Core regions

To further reduce variances between individuals, the functional regions of six rats in each group were superimposed, and the overlapping areas of hip flexion motion and hip extension motion were defined as the core regions.

Statistical analysis

The data were statistically analyzed by SPSS 24.0 (SPSS Inc., Chicago, IL, USA). Differences between groups were analyzed by two-way analysis of variance or Student's *t*-test. A value of $P < 0.05$ was considered significant.

Results

Behavioral function of rats with different types of SCI

There were significant differences in BBB scores between transection and contusion groups during the 2-week observation period ($P < 0.05$). Compared with the transection group, the average BBB score of the contusion group was significantly higher ($P < 0.01$) 1 day after surgery, and these animals were able to slightly move their hindlimbs, which rapidly improved over the following 2 days. In contrast, slight movement of the hindlimb joint was not observed until 1 week in the transection group, when animals in the contusion group showed good hindlimb joint movement. After 2 weeks, the average BBB score in the contusion group exceeded 16 points, with continuous palm movement and coordinated motion. However, it remained below 1 point in the transection groups, and recovery of behavioral function in these rats did not exhibit significant changes with time. Only slight recovery of hindlimb joint movement was achieved in the transection group, which still relied mainly on the strength of the forelimb while walking (**Figure 5**). On the last day, significant differences were observed between the control and contusion groups, contusion and transection groups, and control and transection groups ($P < 0.01$).

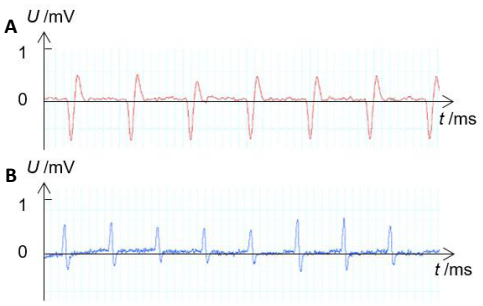

Figure 3 | **Examples of recorded EMG signals.**
(A) EMG of the rectus femoris muscle measured when hip flexion was induced. (B) EMG of the biceps femoris muscle measured when hip extension was induced. X-axis shows the recording time and Y-axis shows the amplitude of EMG signal. EMG: Electromyogram.

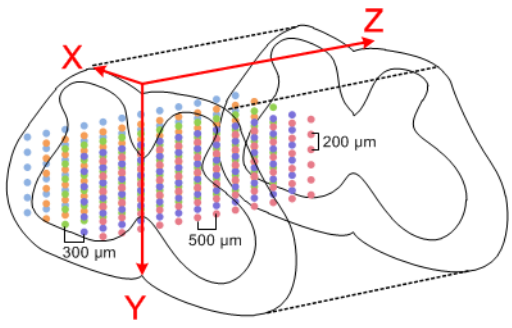

Figure 4 | Sites of functional electrical stimulation.
Stimulation sites were moved at a 300-μm interval along the *X*-axis in the mediolateral direction, at a 200-μm interval along the *Y*-axis in the dorsoventral direction, and at a 500-μm interval along the *Z*-axis in the rostrocaudal direction. Different colors represent sites in different sagittal planes.

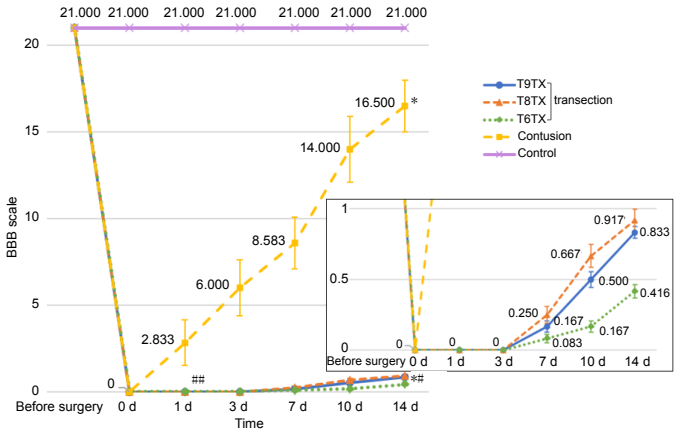

Figure 5 | Basso-Beattie-Bresnahan scores of rats with different types of spinal cord injury.
Data are expressed as the mean ± SD, and analyzed by two-way analysis of variance followed by Student's *t*-test. *P < 0.05, *vs*. control group; #P < 0.05, ##P < 0.01, *vs*. contusion group. Control group: Rats were fed normally for 2 weeks; contusion group: T9 segment was injured with weight drop, followed by 2 weeks of normal feeding; T9TX2, T8TX, T6TX, and T9TX4 groups: T6/T8/T9 transection, followed by 2 or 4 weeks of normal feeding.

Core regions of hip flexion and hip extension in rats with different types of SCI

The functional regions of each group were superimposed, and core regions controlling hip flexion motion and hip extension motion of the right hindlimb were obtained (**Figure 6**). Normalized coordinate ranges are shown in **Table 1**. In the control group, the core region of hip flexion was located in the T13 spine segment (*X*: ~0.63–1.00, *Y*: ~0.64–0.80, *Z*: ~0.07–0.42), while the core region of hip extension was located in the L1 spine segment (*X*: ~0.23–0.63, *Y*: ~0.66–0.83, *Z*: ~0.20–0.53). In the transection group, the core region of hip flexion migrated from the T13 to T12 segment and from the lateral to medial spinal cord. The core region of hip extension migrated from the L1 to T13 segment. Migration distances varied with transection of different segments, but overlapping areas were always found between core regions of the same motion, and the migration trend was consistent. As post-transection time increased, the distance of migration gradually decreased and migration tended to stabilize. However, core regions in contusion and control groups were close to each other, both for hip flexion and hip extension.

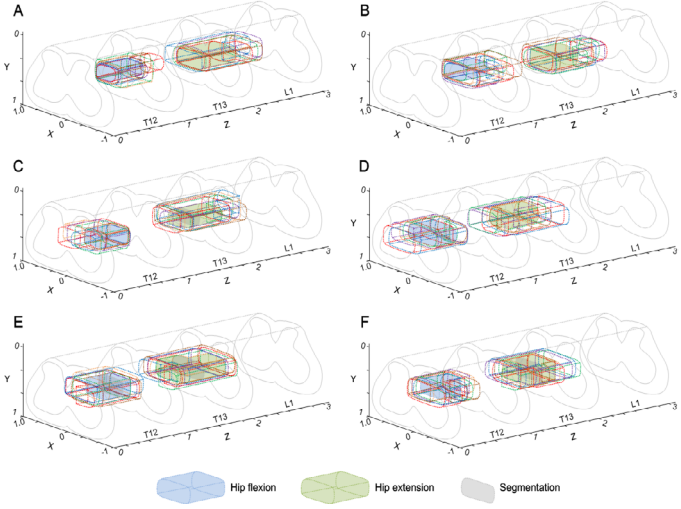

Figure 6 | Core regions of hip flexion and hip extension in rats with different types of spinal cord injury.
Blue-filled areas indicate core regions, while green-filled areas represent core regions of hip extension. Different segments are separated by gray-filled areas. (A–F) Control, contusion, T9TX2, T8TX, T6TX, and T9TX4 groups. Control group: Rats were fed normally for 2 weeks; contusion group: T9 segment was injured with weight drop, followed by 2 weeks of normal feeding; T9TX2, T8TX, T6TX, and T9TX4 groups: T6/T8/T9 transection, followed by 2 or 4 weeks of normal feeding.

Table 1 | Normalized coordinate ranges of hip flexion and extension core regions

	Spine segment	Coordinate ranges		
		X	*Y*	*Z*
Hip flexion core region				
Control	T13	0.58–1.00	0.62–0.83	1.08–1.46
Contusion	T13	0.40–0.95	0.65–0.81	1.03–1.30
Transection				
T9TX2	T12	0.07–0.56	0.66–0.82	0.76–1.00
T9TX4	T12	0.20–0.80	0.62–0.78	0.56–0.68
T8TX	T12	0.40–0.76	0.64–0.80	0.83–1.00
	T13	0.40–0.76	0.65–0.80	1.00–1.17
T6TX	T12	0.40–0.76	0.62–0.76	0.73–0.83
		0.76–0.96	0.62–0.76	0.83–0.98
Hip extension core region				
Control	L1	0.23–0.63	0.64–0.90	2.28–2.78
Contusion	L1	0.12–0.64	0.70–0.87	2.19–2.58
Transection				
T9TX2	T13	0.17–0.62	0.63–0.79	1.88–2.00
T9TX4	T13	0.23–0.63	0.62–0.79	1.73–1.83
		0.63–0.80	0.62–0.79	1.83–2.00
T8TX	T13	0.07–0.76	0.65–0.80	1.91–2.00
	L1	0.23–0.43	0.66–0.82	2.00–2.16
T6TX	T13	0.23–0.93	0.60–0.76	1.92–2.00
	L1	0.23–0.93	0.59–0.74	2.00–2.08

Control group: Rats were fed normally for 2 weeks; contusion group: T9 segment was injured with weight drop, followed by 2 weeks of normal feeding; T9TX2, T8TX, T6TX, and T9TX4 groups: T6/T8/T9 transection, followed by 2 or 4 weeks of normal feeding.

Numbers of active sites and threshold currents in rats with different types of SCI

Compared with the control group, numbers of active sites in the transection groups were greatly reduced, especially for hip extension (P < 0.01). Moreover, in the contusion group, numbers of active sites for hip extension were also reduced, but not as obviously as the transection groups (**Figure 7A**).

Corresponding threshold currents capable of inducing hip flexion and hip extension in each group were analyzed. Average threshold currents in the transection groups and contusion group were increased about 10 μA compared with the control group. Thus, a larger threshold current was needed to induce hindlimb motion after SCI (**Figure 7B**).

Discussion

At its most basic level, SCI can be divided into complete and incomplete injuries (Brown and Martinez, 2019). Transection and weight drop models were used in this experiment to imitate complete and incomplete injuries, respectively (Batista et al., 2019). The segments mentioned in this article are positions of vertebral segments. For example, T9 transection means the transection of spinal cord corresponding to the T9 vertebral segment. The distance of spinous processes of thoracic vertebra is the shortest between the ninth, tenth, and eleventh segments. The spinous processes trend toward the cephalad level above T9, while the tenth has a neutral position and spinous processes trend toward the head below T11 (Shang et al., 2013).

After 2 weeks of observation, BBB scores of the contusion group were much higher than observed in the transection group. According to previous studies (Fehlings and Tator, 1995; Engesser-Cesar et al., 2005), the degree of motor recovery is positively correlated with tissue retention of the lesion center. Indeed, as little as 5% of the residue can cause the hindlimb to recover some or all joint movement; if the residue reaches 10%, the paraplegic animal can stand or even walk. Thus, a small amount of residual fiber can restore great function. The incomplete injury imitated by weight drop resulted in a large amount of fiber residue, which can quickly restore motor function. However, this rapid recovery may not be enough to affect spinal motor function regions. Our results clearly show that the contusion group was very similar to the control group, whereas the transection groups were significantly different from the control group under the same conditions. The common change in all transection groups was migration of the core region. The core region of hip flexion migrated from the T13 to T12 segment, while the core region of hip extension migrated from the L1 to T13 segment. In other words, complete injury may cause the core region to migrate to the injured end. Therefore, we selected the transection SCI model to further study the effects of transection segment and post-transection time on spinal motor function regions.

To avoid the influence caused by similar sections, the T6TX group was added on the basis of T8TX and T9TX, in order. Transection at different segments had less impact on the migration of core regions. The longer the post-transection time, the longer the distance to the injured end and smaller the change. We hypothesized that the underlying reason for migration of core regions is activation of spontaneous healing mechanisms (including remyelination, neural plasticity, and endogenous stem cell activation) after SCI (Jeong et al., 2020). Although these mechanisms are insufficient to produce clinically significant functional recovery, long-term repair can fill cavities formed upon SCI (Oh et al., 2016). The two ends of the lesion can be bridged and, as time goes by, the connection slowly stabilized.

In the present study, SCI rats exhibited deformation in motion of hip flexion and hip extension induced by stimulation. In response to stimulation, both the motion amplitude and angle of joint change became smaller. As time or severity increased, the change became more obvious. These changes were particularly obvious in the transection groups, possibly because the hindlimb muscles were not effectively exercised during the injury period. As a result, the muscles are stiff and affect hindlimb motion, causing the deformation (Jarc et al., 2013). In addition, numbers of transitional motion (hip adduction/abduction) increased, while numbers of normal gait motion (hip flexion/extension) decreased. Threshold currents at all sites were statistically analyzed to obtain the current intensity range required for different motions before and after SCI. The average threshold current was increased in transection and contusion groups compared with the control group, indicating that a larger threshold current is needed for early stimulation after SCI. Stimulating the core region with a suitable current intensity can effectively reduce electrochemical damage.

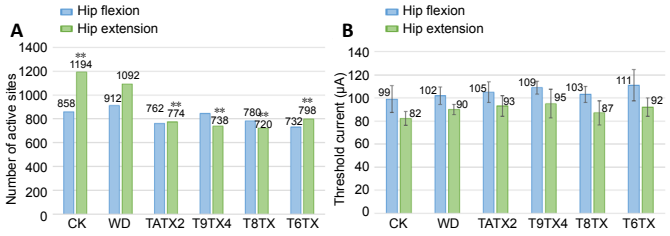

Figure 7 | Numbers of active sites and average threshold currents in rats with different types of spinal cord injury.

(A) Numbers of active sites. (B) Threshold currents. Data are expressed as mean ± SD, and analyzed by two-way analysis of variance followed by Student's *t*-test. $^{**}P < 0.01$, *vs*. control group. Control group: Rats were fed normally for 2 weeks; Contusion group: T9 segment was injured with weight drop, followed by 2 weeks of normal feeding; T9TX2, T8TX, T6TX, and T9TX4 groups: T6/T8/T9 transection, followed by 2 or 4 weeks of normal feeding.

In addition, the use of vertebral segments rather than spinal segments can avoid damage to the spinal cord caused by judging spinal segments *in vivo*, and vertebral segments are easier to measure and mark. In the present study, only the dorsal lamina was cut, because it was difficult to distinguish the spinal cord segment from the surface. To accommodate the use of intraspinal microstimulation, the electrodes should be implanted to a certain depth. It is important to avoid exposure of the lateral spinal cord to reduce unnecessary injury, which also makes it more difficult to determine the spinal cord segment. However, if vertebral segments are used, the stimulation region can be identified as long as the lamina is exposed, thus allowing the spinal cord to be only minimally exposed.

Through these experiments, appropriate stimulation regions and currents were obtained for different experimental conditions. It is hoped that these results will provide a reference for future related experiments (such as rebuilding the motor function of patients suffering from SCI through functional electrical stimulation), improve the accuracy and reliability of electrode implantation, and reduce the damage caused by multiple implants. Although our findings show that SCI can cause migration of motor function regions, it does not rule out the influence of other factors. Future experiments will further investigate the mechanisms leading to migration of core regions in spinal cord and conduct biological analysis of virus tracking to demonstrate the experimental results. In addition, more suitable stimulation positions will be explored.

Acknowledgments: *Thanks for the guidance from Shu-Xin Zhang (retired research scientist of Spinal Cord Society Research Center, USA).*
Author contributions: *Study concepts, definition of intellectual content, and guarantor: XYS; study design: XYS, CLT, LM; literature search, statistical analysis and manuscript preparation: CLT; experimental implementation: CLT, JHS, ZLL; data acquisition and analysis: JHS, ZLL; manuscript editing: JHS, ZLL, LM, ZGW, XYL; manuscript review: XYS, LM, ZGW, XYL. All authors approved the final version of the paper.*
Conflicts of interest: *The authors declare that there is no conflict of interests.*
Financial support: *This work was supported by the National Natural Science Foundation of China, No. 61534003 (to ZGW), 81371663 (to XYS); Opening Project of State Key Laboratory of Bioelectronics in Southeast University (to XYS); the "226 Engineering" Research Project of Nantong Government (to XYS); "Six Talent Peaks" Project, No. SWYY-116 (to XYS) and Postgraduate Research & Practice Innovation Program of Jiangsu Province, No. KYCX18_2424 (to CLT). The funding bodies played no role in the study design, in the collection, analysis and interpretation of data, in the writing of the paper, or in the decision to submit the paper for publication.*
Institutional review board statement: *The study was approved by the Institutional Animal Care and Use Committee of Nantong University, China (approved No. 20190225-008) on February 26, 2019.*
Copyright license agreement: *The Copyright License Agreement has been signed by all authors before publication.*
Data sharing statement: *Datasets analyzed during the current study are available from the corresponding author on reasonable request.*
Plagiarism check: *Checked twice by iThenticate.*
Peer review: *Externally peer reviewed.*

References

Bamford JA, Putman CT, Mushahwar VK (2011) Muscle plasticity in rat following spinal transection and chronic intraspinal microstimulation. IEEE Trans Neural Syst Rehabil Eng 19:79-83.

Bamford JA, Marc Lebel R, Parseyan K, Mushahwar VK (2017) The Fabrication, Implantation, and Stability of Intraspinal Microwire Arrays in the Spinal Cord of Cat and Rat. IEEE Trans Neural Syst Rehabil Eng 25:287-296.

Basso DM, Beattie MS, Bresnahan JC (1996) Graded histological and locomotor outcomes after spinal cord contusion using the NYU weight-drop device versus transection. Exp Neurol 139:244-256.

Batista CM, Mariano ED, Dale CS, Cristante AF, Britto LR, Otoch JP, Teixeira MJ, Morgalla M, Lepski G (2019) Pain inhibition through transplantation of fetal neuronal progenitors into the injured spinal cord in rats. Neural Regen Res 14:2011-2019.

Borrell JA, Frost SB, Peterson J, Nudo RJ (2017) A 3D map of the hindlimb motor representation in the lumbar spinal cord in Sprague Dawley rats. J Neural Eng 14:016007.

Borton D, Bonizzato M, Beauparlant J, DiGiovanna J, Moraud EM, Wenger N, Musienko P, Minev IR, Lacour SP, Millán Jdel R, Micera S, Courtine G (2014) Corticospinal neuroprostheses to restore locomotion after spinal cord injury. Neurosci Res 78:21-29.

Brown AR, Martinez M (2019) From cortex to cord: motor circuit plasticity after spinal cord injury. Neural Regen Res 14:2054-2062.

Capogrosso M, Milekovic T, Borton D, Wagner F, Moraud EM, Mignardot JB, Buse N, Gandar J, Barraud Q, Xing D, Rey E, Duis S, Jianzhong Y, Ko WK, Li Q, Detemple P, Denison T, Micera S, Bezard E, Bloch J, et al. (2016) A brain-spine interface alleviating gait deficits after spinal cord injury in primates. Nature 539:284-288.

Chen Y, Ma L, Du W, Shen X (2017) Measuring functional core regions of hindlimb movement control in the rat spinal cord with intraspinal microstimulation. Sheng Wu Yi Xue Gong Cheng Xue Za Zhi 34:622-626.

Engesser-Cesar C, Anderson AJ, Basso DM, Edgerton VR, Cotman CW (2005) Voluntary wheel running improves recovery from a moderate spinal cord injury. J Neurotrauma 22:157-171.

Fehlings MG, Tator CH (1995) The relationships among the severity of spinal cord injury, residual neurological function, axon counts, and counts of retrogradely labeled neurons after experimental spinal cord injury. Exp Neurol 132:220-228.

Griffin L, Decker MJ, Hwang JY, Wang B, Kitchen K, Ding Z, Ivy JL (2009) Functional electrical stimulation cycling improves body composition, metabolic and neural factors in persons with spinal cord injury. J Electromyogr Kinesiol 19:614-622.

Holinski BJ, Mazurek KA, Everaert DG, Stein RB, Mushahwar VK (2011) Restoring stepping after spinal cord injury using intraspinal microstimulation and novel control strategies. Conf Proc IEEE Eng Med Biol Soc 2011:5798-5801.

Huang ZH, Wang ZG, Lu XY, Li WY, Zhou YX, Shen XY, Zhao XT (2016) The principle of the micro-electronic neural bridge and a prototype system design. IEEE Trans Neural Syst Rehabil Eng 24:180-191.

Jackson A, Zimmermann JB (2012) Neural interfaces for the brain and spinal cord--restoring motor function. Nat Rev Neurol 8:690-699.

Jarc AM, Berniker M, Tresch MC (2013) FES control of isometric forces in the rat hindlimb using many muscles. IEEE Trans Biomed Eng 60:1422-1430.

Jeong SK, Choi I, Jeon SR (2020) Current status and future strategies to treat spinal cord injury with adult stem cells. J Korean Neurosurg Soc 63:153-162.

Musienko P, van den Brand R, Maerzendorfer O, Larmagnac A, Courtine G (2009) Combinatory electrical and pharmacological neuroprosthetic interfaces to regain motor function after spinal cord injury. IEEE Trans Biomed Eng 56:2707-2711.

Nakae A, Nakai K, Yano K, Hosokawa K, Shibata M, Mashimo T (2011) The animal model of spinal cord injury as an experimental pain model. J Biomed Biotechnol 2011:939023.

Oh SK, Choi KH, Yoo JY, Kim DY, Kim SJ, Jeon SR (2016) A phase III clinical trial showing limited efficacy of autologous mesenchymal stem cell therapy for spinal cord injury. Neurosurgery 78:436-447.

Saigal R, Renzi C, Mushahwar VK (2004) Intraspinal microstimulation generates functional movements after spinal-cord injury. IEEE Trans Neural Syst Rehabil Eng 12:430-440.

Shang YL, Li YF, Ning YF, Lv YS, Li XS, Zhao J, Li CC (2013) Anatomy reference location for model of SCI rats. Jiepouxue Zazhi 35:412-414.

Shen XY, Wang ZG, Lü XY, Li WY, Zhao XT, Huang ZH (2010) Neural function rebuilding on different bodies using microelectronic neural bridge technique. Dongnan Daxue Xuebao: Yingwen Ban 26:523-527.

Shen XY, Wang ZG, Lü XY, Jiang ZL, Zhao XT, Huang ZH (2012) Experimental research on rebuilding motive functions of rat using microelectronic neural bridge. Dongnan Daxue Xuebao: Ziran Kexue Ban 42:843-847.

Song W, Duan HM, Rao JS, Zhao C, Yang ZY (2015) Behavioral and morphological changes of different spinal cord injury rat models. Zhongguo Zuzhi Gongcheng Yanjiu 19:7920-7925.

Wang ZG, Lü XY, Li WY, Wang HL, Zhang ZY, Wang YF, Cui W (2005) Study of microelectronics for detecting and stimulating of central neural signals. In: Proceedings. 2005 First International Conference on Neural Interface and Control, 2005, pp 192-195. Wuhan.

Zhou ZL (2013) Comparison of mesenchymal stem cells from human bone marrow and adipose tissue for the treatment of spinal cord injury. Guangzhou: Southern Medical University.

C-Editor: Zhao M; S-Editors: Yu J, Li CH; L-Editors: Deusen AV, Yu J, Song CP; T-Editor: Jia Y